MODELING SURFACE TENSION AND WALL ADHESION IN MOLD FILLING PROCESS

N. Hatami[1], R. Babaei[1]and P. Davami[2]
n-hatami@SUTCAST.com
Date of Receive: January 2008 Date of Acceptance: May 2008

[1] Razi Metallurgical Research Center, Tehran, Iran
[2] Department of Material Science and engineering, Sharif University of Technology, Tehran, Iran

Abstract: *In this study an algorithm for mold-filling simulation with consideration of surface tension has been developed based on a SOLA VOF scheme. As the governing equations, the Navier-Stokes equations for incompressible and laminar flows were used. We proposed a way of considering surface tension in mold-filling simulation. The proposed scheme for surface tension was based on the continuum surface force (CSF) model; we could confirm the remarkable effectiveness of the surface tension by experiment which concluded in very positive outcome.*

Keywords: *Simulation, Surface Tension, SOLA-VOF.*

1. INTRODUCTION

Molecules of Fluid on, or near liquid surfaces experience uneven molecular forces of attraction. This causes the liquid surfaces to possess an elastic skin (surface tension). Surface tension is an inherent characteristic of material interfaces because abrupt changes in molecular forces occur when fluid properties change discontinuously. Surface tension results in a microscopic localized "surface force". These forces exert themselves on fluid elements at interfaces in both the normal and tangential directions. Fluid interfacial motion induced by surface tension plays a fundamental role in many natural and industrial phenomena. For example, capillarity, low-gravity fluid flow, hydrodynamic stability, surfactant behaviour, cavitation, and droplet dynamics in clouds and in fuel sprays used in internal combustion engines [1-10] are examples. A Detailed analysis of these processes typically involves the use of numerical models to aid in understanding the resulting non-linear fluid flows. In 1988 Sethian and Osher [13] proposed an LSM (Level Set Method). In this method, a continuous function is introduced over the whole computational domain. This function has the properties of a distance function indicating the shortest distance to the interface. In 1992, Brackbill et al. proposed the CSF method for modeling surface tension [11]. This model interprets surface tension as a continuous, three-dimensional effect across an interface, rather than as a boundary value condition on the interface. In 1994, Sussman, Osher and Smereka extended the LSM method to a compressible two-phase flow. In 1998, M. W. Williams et al. proposed the CST (Continuum Surface Tension) method [16]. This method generated better than second-order accurate approximations to the curvature of circular and spherical interfaces. In 2002, Marianne M. Francois proposed the GFM (Ghost Fluid Method) and compared it with CSF method [12]. In the same year, Berthelsen showed that the LSM and CSF methods are equivalent [15].
In this study, the CSF method was selected as the numerical method because previous methods have suffered from difficulties in modeling topologically complex interfaces which have surface tension.

2. PHYSICAL MODEL

The surface stress boundary condition at an interface between two fluids (labeled 1 and 2) is [17]:

$$(P_1 - P_2 + \sigma K)\hat{n}_i = (\tau_{1ik} - \tau_{2ik})\hat{n}_k + \frac{\partial \sigma}{\partial x_i} \qquad (1)$$

Where σ is the fluid surface tension coefficient (in units of force per unit length), P_α is the pressure in fluid α for α = 1; 2, $\tau_{\alpha ik}$ is the viscous stress tensor, n_i is the unit normal (into fluid 2) at the interface, and K is the local surface curvature $R_1^{-1} + R_2^{-1}$, where R1 and R2 are the

principal radii of curvature of the surface. σ can only have a surface gradient; this would be, perhaps, more clearly indicated by replacing $\frac{\partial \sigma}{\partial x_i}$ in (1) by $(\delta_{ik} - \hat{n}_i \hat{n}_k)\frac{\partial \sigma}{\partial x_k}$. The gradient along a direction normal to the interface, ∇N, is:

$$\nabla N = \hat{n}(\hat{n}.\nabla) \tag{2}$$

The surface tension, σ, may vary along the interface and its gradient tangent to the interface is defined using the differential surface operator, ∇S,

$$\nabla S = \nabla - \nabla N \tag{3}$$

In this study, a one–Phase fluid flow model was used, the fluid labeled 2 is empty and its density is zero. Projecting (1) along the unit normal, $\hat{n}$, and tangent, $\hat{t}$, results in scalar boundary conditions for the fluid pressure in directions both normal and tangent to the interface respectively. While the normal stress boundary condition can be satisfied at the interface between the two fluids that at rest, the tangential stress boundary condition requires the fluid to be in motion. Surface tension manifests itself in the normal direction as a force, σk, whitch drives fluid surfaces towards a minimal energy state characterized by the configuration of a minimum surface area. Spatial variations in the surface tension coefficient go along the interface $(\frac{\partial \sigma}{\partial s})$, because fluids flow from regions of lower to higher surface tension. In our model, the normal boundary condition for interfaces is modeled where the surface tension coefficient is constant. This condition is reduced to Laplace's formula for the surface pressure (PS) where the fluid pressure jumps across an interface under surface tension,

$$P_S \equiv P_2 - P_1 = \sigma k \tag{4}$$

Surface pressure is therefore proportional to the curvature (k) of the interface. Since surface tension results in a net normal force directed towards the centre of curvature of the interface, the highest pressure is in the fluid medium on the concave side of the interface.

3. MATHEMATICAL MODEL (CSF METHOD)

Surface tension contributes to surface pressure (4), which is the normal force per interfacial unit area. We consider interfaces between fluids because they have a constant surface tension coefficient. This force has only normal components; therefore, the surface force per interfacial unit area can then be written as:

$$\vec{F}_{Sa}(\vec{x}_S) = \sigma k(\vec{x}_S)\hat{n}(\vec{x}_S) \tag{5}$$

Where $K(\vec{x}_S)$ is the curvature considered positive if the center of curvature is in fluid 2, and $\hat{n}(\vec{x}_S)$ is the unit normal to A at $\vec{x}_S$, assumed to point into fluid 2 (Fig. 1). Consider two fluids, fluid 1 and fluid 2, separated by an interface at time t. Two fluids are distinguished by some characteristic function, $C(\vec{x}_S)$,

$$C(\vec{x}_S) = \begin{cases} C_1 & InFluid1 \\ C_2 & InFluid2 \\ < C >= (C_1 + C_2)/2 & Interface \end{cases} \tag{6}$$

that changes discontinuously at the interface.

The CSF Method originally considered replacing the discontinuous characteristic function with a smooth variation of fluid color $\widetilde{C}(\vec{x})$ from C1 to C2 over a distance of $\vartheta(h)$ where h is a length comparable to the resolution afforded by a computational mesh with spacing Δx. This replaces the boundary-value problem at the interface with an approximate continuous model, which mimics the problem specification in a numerical calculation, where one specifies the values of c at the grid points and interpolates between them. It is no longer appropriate to apply a pressure jump induced by the surface tension at an interface. Rather, surface tension should be considered to act everywhere within the transition region. Consider the volume force, $\vec{F}_{Sv}(\vec{x}_S)$, that gives the correct surface tension force per interfacial unit area, $\vec{F}_{Sa}(\vec{x}_S)$, as $h \to 0$. We identify this volume force for finite h as

$$\vec{F}_{Sv}(\vec{x}) = \sigma k(\vec{x})\frac{\nabla \widetilde{C}(\vec{x})}{[C]} \tag{7}$$

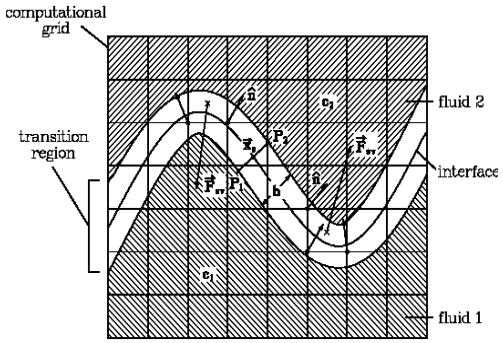

Fig. 1. Mathematical method.

Where [c] is the jump in color, [c] $= C_2 - C_1$.
The reader is reffered to ref[11] for a detailed discussion of CSF method.

4. NUMERICAL MODEL

4.1. Color Function

For tracing the free surfaces, VOF technique is used. Also F (0<F<1) is used as the characteristic function in the CSF method. When computational cells are full, F=1 becomes zero since there is no fluid in the cell. In other research references [11] for example, density functions have been the chosen characteristic function. Consider at grid points,

$$\widetilde{C}(\vec{x}) = F(\vec{x}) \tag{8}$$

Therefore the volume force is still given by (6). The transition region thickness is then of the order of the grid spacing, and at the points outside the transition region, $\widetilde{C}(\vec{x})$ has the values 0, 1 in fluids 1, 2, respectively. The interface between the fluids is given by the surface $F(\vec{x}) = \frac{1}{2}(1+0) = \frac{1}{2} = < F >$.

One can multiply the integrand on the right side of (6) by the function $g(\vec{x}) = \frac{\widetilde{C}(\vec{x})}{< C >}$ because of the interface $\vec{x} = \vec{x}_S$ and $g(\vec{x}) = 1$. For incompressible flow, we use $\widetilde{C}(\vec{x}) = F(\vec{x})$, therefore $g(\vec{x})$ is given by

$$g(\vec{x}) = \frac{F(\vec{x})}{< F >} \tag{9}$$

And the volume force in (6), when multiplied by $g(\vec{x})$, becomes:

$$\vec{F}_{SV}(\vec{x}) = \sigma k(\vec{x}) \frac{\nabla \vec{F}(\vec{x}) \vec{F}(\vec{x})}{[F] < F >} \tag{10}$$

With this modification, fluid acceleration due to surface tension is modeled as a volume force density. Thus, if this force is substituted into the Navier-Stoks formulation, we have:

$$\frac{d\vec{u}}{dt} \equiv \frac{\sigma k \nabla F . F}{[F] < F > \rho} \tag{11}$$

4.2. Evaluation of Curvature

The curvature of a surface A at $\vec{x}_S$, k, is calculated from

$$K = -(\nabla . \hat{n}) \tag{12}$$

where, $\hat{n}$ is the unit normal to the surface. In the CSF model, the interface is replaced by nested surfaces of constant color, this normal is the gradient of the mollified color function,

$$\vec{n}(\vec{x}) = \nabla \widetilde{F}(\vec{x}) \tag{13}$$

The unit normal is

$$\hat{n}(\vec{x}) = \frac{\nabla \widetilde{F}(\vec{x})}{\left| \nabla \widetilde{F}(\vec{x}) \right|} \tag{14}$$

Therefore, $K.\nabla \widetilde{F}(\vec{x})$ is needed to evaluate the surface volume force, which is given by,

$$K.\nabla \widetilde{F} = -\vec{n}(\nabla . \hat{n}) \tag{15}$$

Since $\nabla \widetilde{F}$ is not at zero in the transition region, the surface volume force is also not at zero in the transition region.

4.3. Discrete Equations

We have used the MAC method to discrete equations. In this method the F Function resides at cell's centers. The curvature K therefore will also be cell-centered. We also chose to locate $\vec{F}_{SV}$ at cell centers. The normal vectors at the cell centers must be interpolated from nearby cell faces in the MAC method

5. WALL ADHESION (BOUNDARY CONDITION

The effects of wall adhesion on fluid interfaces in contact with rigid boundaries in equilibrium can be estimated easily within the framework of the CSF model in terms of θ_{eq}, the equilibrium contact angle between the fluid and wall. The angle θ_{eq} is called the static contact angle because it is experimentally measured when the fluid is at rest. In Fig. 2, if $0 < \theta_{eq} < 90$, the fluid will wet the wall and if $90 < \theta_{eq} < 180$, it will also separate itself from the wall. To calculate the static contact angle we can write (Fig. 2)

$$\sigma_{12} Cos\theta_{eq} + \sigma_{31} = \sigma_{32} \quad InEquilibrium$$
$$\Rightarrow Cos\theta_{eq} = \frac{\sigma_{32} - \sigma_{31}}{\sigma_{12}} \tag{16}$$

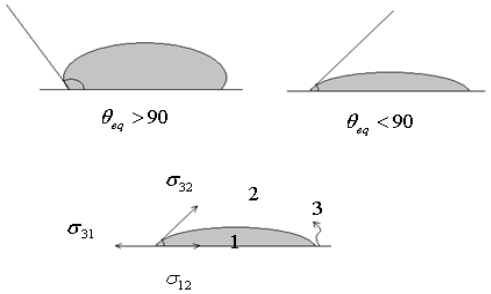

Fig. 2. Contact angle.

Where, σ_{12}, σ_{31} and σ_{32} are surface tension coefficients between materials labeled from 1 to 3. The equilibrium contact angle is not simply a material property of the fluid. It also depends on the walls smoothness and geometry.
The interfaces normal at points on the wall is

$$\hat{n} = \hat{n}_{wall} Cos\theta_{eq} + \hat{n}_t Sin\theta_{eq} \quad (17)$$

Where $\hat{n}_t$ lies in the wall and is normal to the contact line between the interface and the wall, and $\hat{n}_t$ is the unit wall normal directed into the wall. The unit normal $\hat{n}_t$ is computed by using (13). Wall adhesion boundary conditions are more complex when the contact lines are in motion, i.e., when the fluid in contact with the wall is moving relative to the wall. The equilibrium of the wall adhesion boundary condition in (15) may have to be generalized by replacing θ_{eq} with a dynamic contact angle, θ_d, that depends on local fluid and wall conditions.

6. STABILITY

The explicit treatment of surface tension is stable when the time step resolves the propagation of capillary waves [19],

$$\Delta t_s < \left(\frac{< \rho > (\Delta x)^3}{2\pi\sigma} \right)^{1/2} \quad (18)$$

Where, $< \rho >= (\rho_1 + \rho_2)/2$
This condition should be added to other time steps in the limitation conditions in the algorithm of fluid flow modeling.

7. NUMERICAL RESULTS

To illustrate the flexibility and accuracy of the model, we present the results of several standard static and dynamic problems with surface tension.

7.1. Static Liquid Drop Test

In the absence of viscous, gravitational, or other external forces, surface tension causes a static liquid drop to become spherical. Laplace's formula for a drop surrounded by a background fluid at 100005 (Pa) pressure, (4), gives the internal drop pressure defined by

$$P = K\sigma = \frac{2\sigma}{R} \quad (19)$$

Where, R is the drop radius. Results in the Cartesian geometry using a tree-dimensional

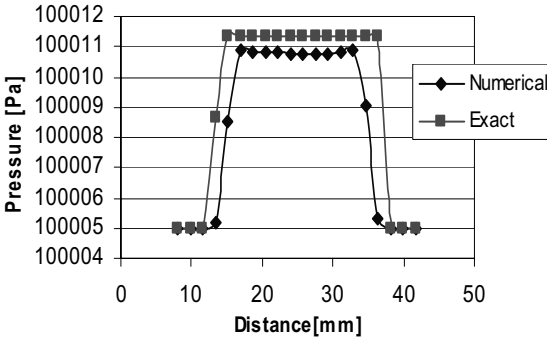

Fig. 3. Comparison between numerical results and exact Pressure of Static liquid drop.

$50 \times 50 \times 50$ computational grid (Δx=2mm) are compared with (17). The fluid drop radius is R = 10 and 15 (cm), density = 1000 (Kg/m^3), background density = 0 (Kg/m^3), and surface tension coefficient = 0.07275 (N/m). The pressure jump is 100005+$K\sigma$ (N/m^2). This value is compared with the mean computed drop pressure obtained with the CSF model. The sum is done over the computational cells lying within the drop that has fluid. The relative error between the theoretical and computed drop pressure is given by,

$$\%ERR = \frac{\left(\sum_{i=1}^{N} P_i\right)/N - K\sigma}{K\sigma} \quad (20)$$

where, N is the number of cells within the drop. Table 1 illustrates computational errors in two value of drop radius to the mesh size ratio

Table 1. Computational Errors

Radius /mesh size	%Error
10	0.219
15	0.1357

Fig. 3 illustrates variation of theoretical and numerical drop pressure through the drop diameter when the drop radius to the mesh size ratio is 10 and simulation time is 0.2 s.

7.2. Square Drop Test

When a drop is initially square, it responds to unbalanced surface tension forces. The mesh size, computational grid and liquid properties are the same as in the previous test. Gravity is neglected and the Square length is 32 mm. Results are shown at a sequence of times, t=0, 0.15, 0.2, 0.3, 0.4, 0.5, 0.7, 0.8, and 1.1 s in fig.4. At t=1.1 s, the drop is nearly circular in cross section (minimum energy state).

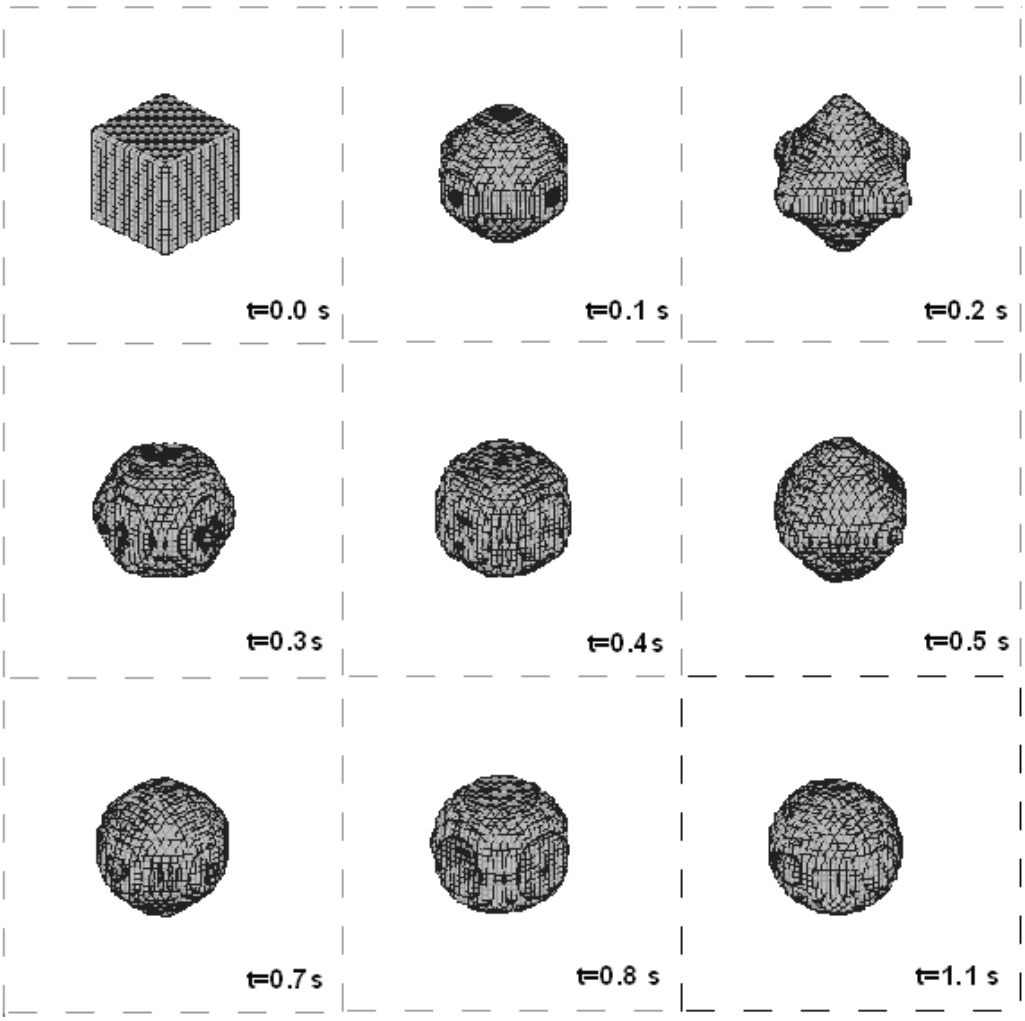

Fig. 4. Variation of Square drop shape.

7.3. Mold filling test

In this test, we used pure melt Mg (density = 1580[kg/m^3], surface tension coefficient = 0.59 [N/m]). The computational grid is 77×14×64 and the mesh size is 4 mm. The contact angle equals 150°. As shown in Fig. 5, the effects of surface tension were small in the mold filling, but modeling surface tension makes for better results. The free surface is flatter when surface tension is modeled (minimum energy state) and fluid flow modeling results are better as well.

8. CONCLUSIONS

Through a detailed study of the properties of CSF method for modeling of surface tension at fluid-gas interface, we have a deeper understanding of the molten metal flow with surface tension. The numerical method is used to solve for the velocity and pressure and the advection of free surface is described. We have detailed the boundary condition used and discussed numerical stability issue. Many types of free surface problems can now be solved with the aid of our program, as can be seen one of them is casting. Our numerical results were compared with experiments and have good agreements.

ACKNOLEDGMENTS

This project was supported by the Razi Metallurgical Research Center. The authors would like to acknowledge fruitful conversation with our colleagues A. Mirak, M Dadashzadeh, K. Asgharie.

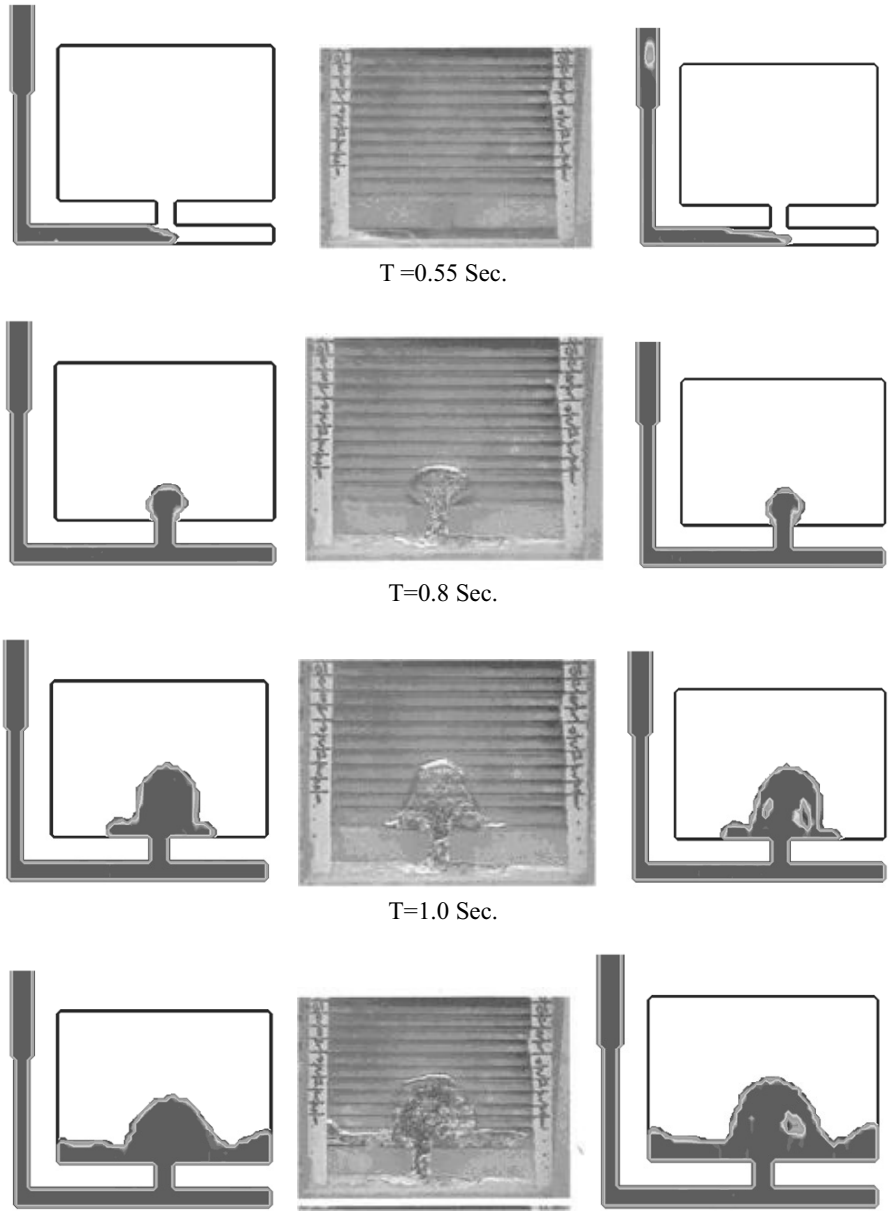

Fig. 5. Comparison between simulation and experiments in mold filling, a-simulation with surface tension model, b- experimental, c- simulation without surface tension model.

REFERENCES

1. Levich, V. G.: Physicochemical Hydrodynamics. Prentice-Hall, Englewood Cli_s, NJ, 1962.
2. Lamb, H.: Hydrodynamics. Cambridge University Press, Cambridge, 1932, 6th edition.
3. Ostrach, S: Ann. Rev. Fluid Mech. 14, 313 (1982).
4. Myshkis, A. D., Babskii, V. G., Kopachevskii, N. D., Slobozhanin, L. A., and Tyuptsov, A. D.: Low-Gravity Fluid Mechanics. Springer-Verlag, New York, 1987.
5. Drazin, P. G. and Reid, W. H.:

Hydrodynamic Stability. Cambridge University Press, Cambridge, 1981.
6. Oguz, H. N. and Sadhal, S. S.: J. Fluid. Mech. 194, 563 (1988).
7. Gaver, D. P., III, and Grotberg, J. B.: J. Fluid. Mech. 213, 127 (1990).
8. Batchelor, G. K.: an Introduction to Fluid Dynamics. Cambridge University Press, Cambridge, 1967.
9. Pruppacher, H. R. and Klett, J. D.: Microphysics of Clouds and Precipitation. Reidel, Dordrecht, Holland, 1978.
10. Oran, E. S. and Boris, J. P.: Numerical Simulation of Reactive Flow. Elsevier, NewYork, 1987.
11. Brackbill, J. U., Kothe, D. B., and Zemach, C.: A Continuum Method for Modeling Surface Tension. Journal of Computational Physics 100, 1992, pp.335-354.
12. Francois, M. M., Kothe, D. B., Cummins, S. J.: Modeling Surface Tension Using a Ghost Fluid Technique Within a Volume of Fluid Formulation. Los Alamos, National Laboratory, NM 87545, U.S.A.
13. Osher, S. & Sethian, J. A.: Fronts propagating with curvature-dependentspeed (Algorithms based on hamilton-jacobi formulations). Journal of Computational Physics 79, 1988, pp.12–49.
14. Sussman, M., Smereka, P. & Osher, S: A level set approach for computing solutions to incompressible two-phase .Flow. Journal of Computational Physics. 1994, pp.146–159.
15. Berthelsen, P. A: A Short Introduction to the Level Set Method and Incompressible Two-Phase Flow. A Computational Approach, Department of Applied Mechanics, NTNU, A rough draft, 2002.
16. Williams, M. W., Kothe, D. B., Puckett, E. G.: Accuracy and Convergence of Continuum Surface Tension Models. Los Alamos, National Laboratory, NM 87545, U.S.A.
17. Landau, L. D. & Lifshitz, E. M.: Fluid Mechanics. Pergamon Press, New York, 1959.
18. Levich, V.G. & Krylov, V. S.: Ann. Rev. Fluid Mech. 1, 293 ,1969.
19. De Boor, C.: A Practical Guide to Splines. Springer-Verlag, New York, 1967.
20. Tavakoli, R.: fluid flow simulation in low pressure die cast. Msc thesis, Sharif University of Technology, 2003.
21. Babaei, R., Abdollahi, J., Homayonifar, P., Varahram, N. & Davami, P.: Improved Advection Algorithm of Computational Modeling of Free Surface Flow Using Structured Grids. Computer Methods in Applied Mechanics and Engineering, V.195, 2006, PP.775-795.